SINGLE IMPULSE MEASUREMENT OF A COAXIAL PULSED PLASMA THRUSTER

Masahiko Kameoka* **and Haruki Takegahara†**
Tokyo Metropolitan Institute of Technology, Dept. of Aerospace Eng.
6-6, Asahigaoka, Hino, Tokyo 191-0065, JAPAN
kame@ep.isas.ac.jp

Yukio Shimizu‡ **and Kyoichiro Toki†**
Institute of Space and Astronautical Science, Japan
3-1-1, Yoshinodai, Sagamihara, Kanagawa 229-8510, JAPAN

IEPC-03-0093

Abstract

Since pulsed plasma thrusters generate a very small impulse, so one cannot measure its magnitude easily. Recently, micro-thrusters were paid attention, and researches about a method of small impulse measurement have been increasing. It is important for thrusters operating pulsed mode to measure every impulse bit. In this study, we designed a torsion-type thrust stand which enables to measure a single shot impulse of our newly designed a coaxial pulsed plasma thruster. Our torsion type thrust stands are suspended from the chamber ceiling by a pair of wires or a C-section pipe for its rotation axis. We also analyzed the motion of the thrust stand to achieve the reasonable S-N ratio. Furthermore, we measured for comparison the impulse bit of our coaxial PPT using the target pendulum which is the conventional method of a small impulse measurement.

Introduction

Recently, the size and the weight of satellites are decreased because of cost reduction, avoiding the risk and compressing the development period. The small-sized and the low thrust thrusters called microthrusters have been received a great deal of attention. Several organizations have researched and developed the microthrusters[1], a Pulsed Plasma Thruster (PPT) is a typical example[2-3]. The research concerning the method of a small impulse measurement has been performed as well as development microthrusters[4-9]. Also in ISAS, a PPT research and development have begun, and a coaxial configuration was selected. The impulse level of the PPT is *m*Ns order, and it is difficult to measure accurately. In Japan, most of a small impulse measurement has been performed by using a target pendulum. But this method is indirect and not a single impulse measurement. For pulsed mode thrusters, it is important to measure a single impulse bit. We designed the torsion-type thrust stand which enables a single impulse measurement, and applied it to our coaxial PPT performance evaluation from the calibration result.

*Graduate Student.
†Professor, Member AIAA.
‡Research Engineer.

PPT

Figures 1 and 2 show the appearance of the PPT and the cross section of the thruster head, respectively. The size of the PPT is about 100×80×80mm including capacitors. The coaxial thruster head, which consists of an anode, a cathode, an ignitor, and a propellant has an outer diameter of 14mm. The ignitor, which is placed outermost, is not a conventional pin-type ignitor but a cylindrical-type because of the durability against the erosion. The shape of the ignitor is made like a nozzle which is sharp near the cathode, and the ignition energy is concentrated so that the electric field between the ignitor and the cathode becomes strong. The capacitor bank consisting of three paralleled mica capacitors has a total capacitance of 4.4*m*F and a chargeable voltage of 4kV. PTFE is selected as the propellant.

Figure 3 shows the current waveform measured by a rogowski coil.

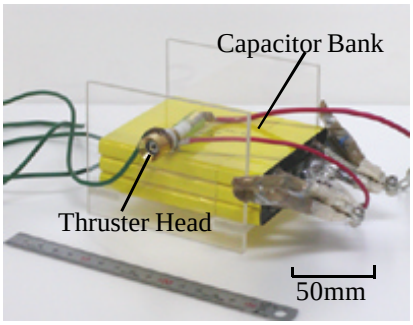

Fig. 1 Coaxial PPT.

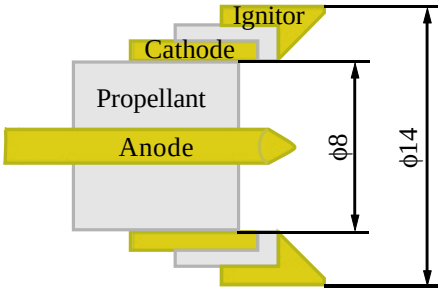

Fig. 2 Thruster Head.

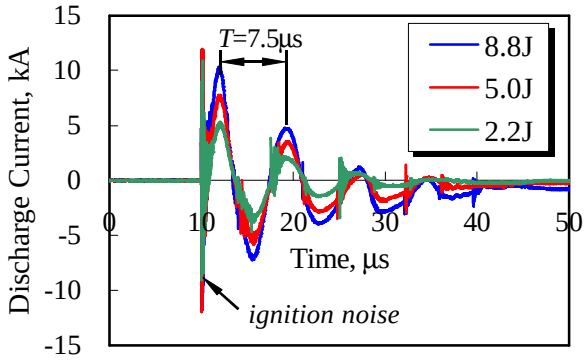

Fig. 3 Current Waveform.

Thrust Stand

Since the impulse level of the PPT is *m*Ns order, it is difficult to measure accurately. In this study, we selected the torsion-type thrust stand for measurement of the impulse bit of the PPT. Figure 5 (c) shows the measurement principle of the torsion-type thrust stand, when the PPT installed on the thrust stand operates, the thrust stand rotates around its rotation axis by the torque resulted from the impulse bit of the PPT. We measured the displacement of the thrust stand with the laser displacement meter, and we could evaluate the impulse of the PPT from the calibration result.

Our torsion-type thrust stands are suspended from the ceiling of the vacuum chamber as shown in Figs. 4 and 5. We designed the thrust stand A first, and imploved it as the thrust stand B by improved some point. The thrust stand A is suspended by a pair of piano wires. Figure 4 (b) shows the way how to suspend by wires. There is a small plate between the main body and the ceiling of the vacuum chamber, the main body is suspended from the small plate with four wires, and the small plate is suspended from the ceiling of the vacuum chamber with a pair of wires. The thrust stand B is suspended by the C-section pipe which is shown in Fig. 5 (b) The displacement of both thrust stands was measured with the laser displacement meter.

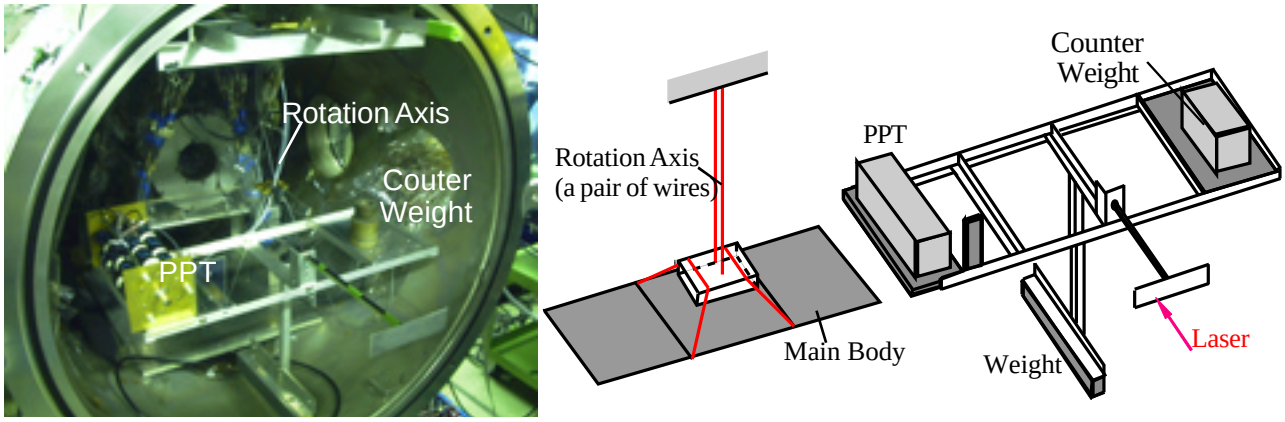

(a) Appearance (b) Way to suspend (c) Main Body

Fig. 4 Thrust Stand A.

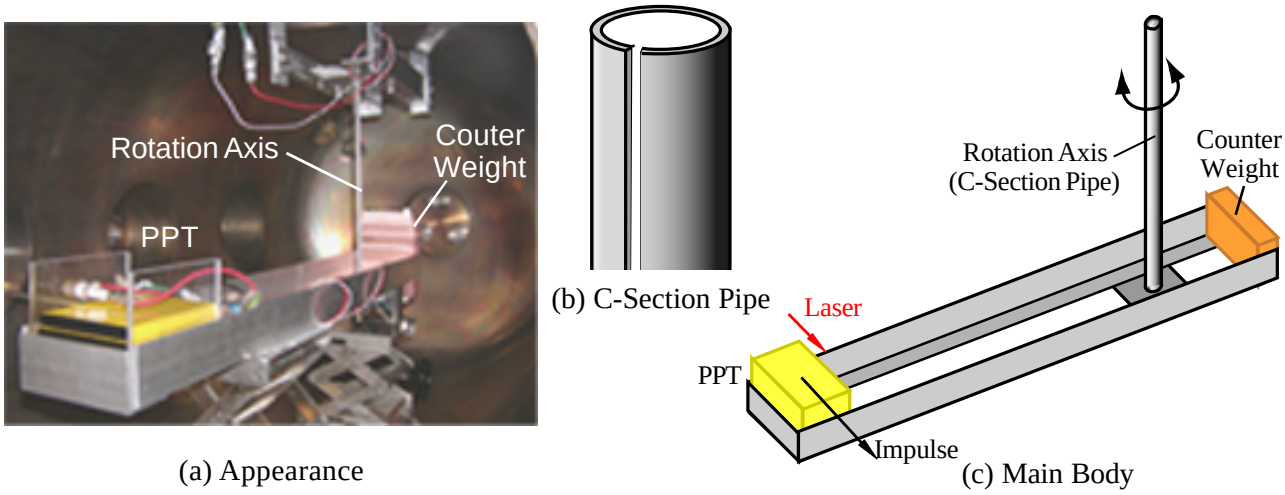

(a) Appearance (c) Main Body

Fig. 5 Thrust Stand B.

Figure 6 shows the output of the displacement meter when we measured the impulse bit with the thrust stand A. One can find that the signal-to-noise ratio (S-N ratio) is insufficient. Therfore we analyzed the motion of the thrust stand to obtain a reasonable S-N ratio, and we eventually found the guideline for the design of our new thrust stand.

Figure 7 shows the analytical model corresponding to the thrust stand A. This model consists of a main body with thruster installed, a stabilizing weight connected under the main body, and the light weight object simulating wires between the main body and the ceiling of the vacuum chamber, and three objects are connected with

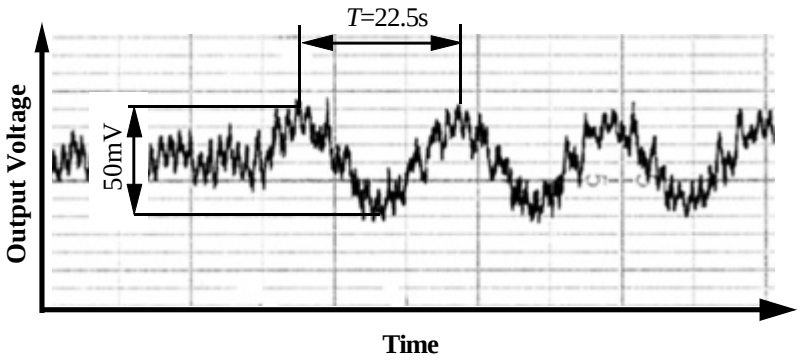

Fig. 6 Displacement of the Thrust Stand A.

rods. The counter weight is also installed on the main body to balance the main body and the PPT. When the PPT generates impulse, the thrust stand rotates around the rotational axis, namely the rod.

We analyzed two motions of the thrust stand, which are the rotation motion and the pendulum motion. The governing equations are as follows

(i) Equations describing the rotation motion

$$\begin{cases} J_1\ddot{q}_1 + c_1\dot{q}_1 + (k_1+k_2)q_1 - k_2q_2 = 0 \\ J_2\ddot{q}_2 + c_2\dot{q}_2 - k_2q_1 + (k_2+k_3)q_2 - k_3q_3 = 0 \\ J_3\ddot{q}_3 + c_3\dot{q}_3 - k_3q_2 + k_3q_3 = 0 \\ q_1(0) = q_2(0) = q_3(0) = \dot{q}_1(0) = \dot{q}_3(0) = 0 \\ \dot{q}_2(0) = \dfrac{I_b l_t}{J_2} \end{cases} \quad (1)$$

$$x_t = l_m q_2$$

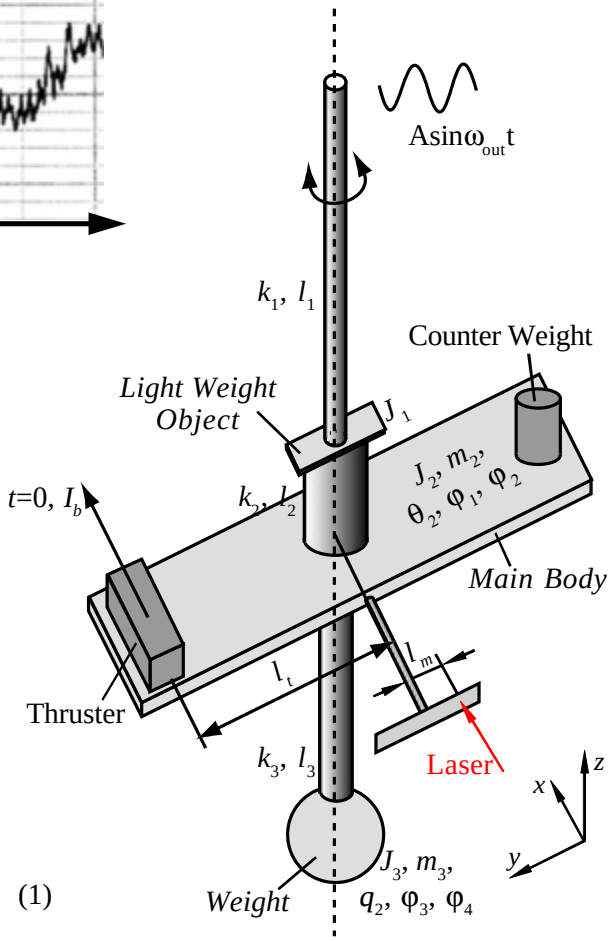

Fig. 7 Analytical Model.

(ii) Equations describing the pendulum motion

$$\begin{cases} (m_2+m_3)(l_1+l_2)\ddot{j}_1 + m_3l_3\ddot{j}_3 + (m_2+m_3)gj_1 = \dfrac{A}{l_1+l_2}\sin w_{out}t \\ (l_1+l_2)\ddot{j}_1 + l_3\ddot{j}_3 + gj_3 = \dfrac{A}{m_3l_3}\sin w_{out}t \\ m_2l_2\ddot{j}_2 + m_3l_3\ddot{j}_4 + (m_2+m_3)gj_2 = \dfrac{A}{l_2}\sin w_{out}t \\ l_2\ddot{j}_2 + l_3\ddot{j}_4 + gj_4 = \dfrac{A}{m_3l_3}\sin w_{out}t \\ j_1(0) = j_2(0) = j_3(0) = j_4(0) = \dot{j}_3(0) = \dot{j}_4(0) = 0 \\ \dot{j}_1(0) = \dfrac{I_b}{m_2(l_1+l_2)} \\ \dot{j}_2(0) = \dfrac{I_b}{m_2l_2} \end{cases} \quad (2)$$

$$x_p = (l_1+l_2)j_1 + l_2j_2$$

The initial condition of these pendulum systems is stationary and the impulse is generated on the main body, object 2. In the equation for the pendulum motion, object 1 ignores the mass, and has a role of a fulcrum. Figure 8 shows the double pendulums consisting of object 2 and 3, but the fixed fulcrum shown in Fig. 8 (a) is the ceiling of the vacuum chamber and another shown in Fig. 8 (b) is the object 1. The displacement x_p comes from the pendulum motion is superimposed with the two displacements as usually found in a double pendulum problem.

The displacement x measured with the laser displacement meter is superimposed by the displacement coming from the rotation motion x_t and that coming from the pendulum motion x_p, so it can be found as the following equation.

$$x = x_t + x_p \qquad (3)$$

Figure 9 shows the simulation result.

As the next step, to find the most effective way of increasing the S-N ratio we changed some parameters shown in Fig. 7, for example l_1, J_2, and so on, and examined the change of the S-N ratio. Figure 10 shows the some of

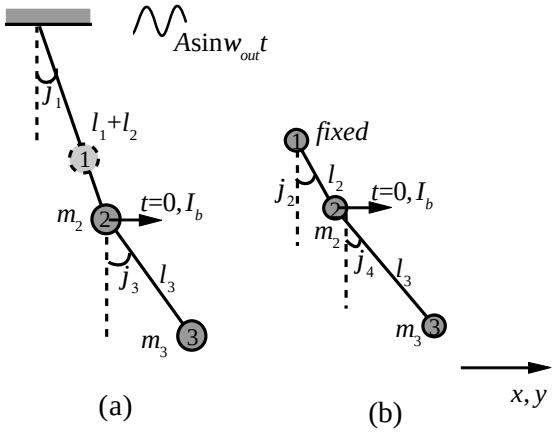

Fig. 8 Pendulum Motion.

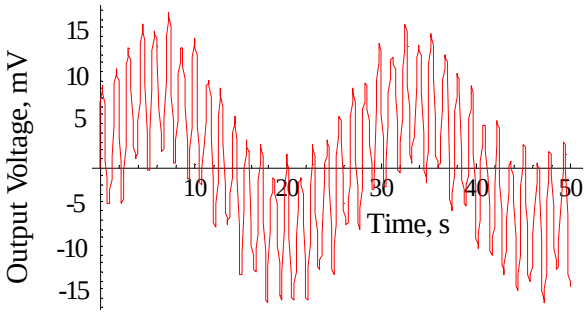

Fig. 9 Simulation Result.

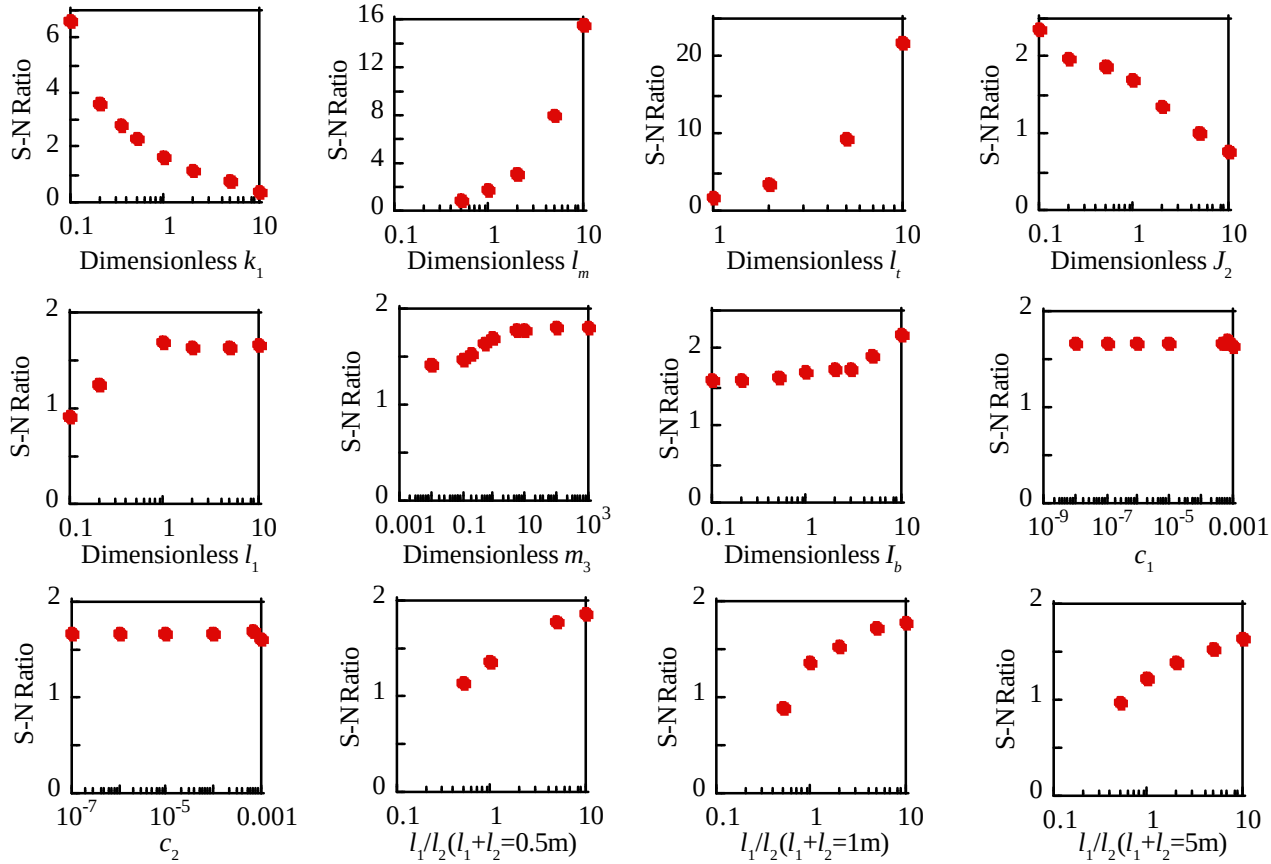

Fig. 10 Variation of S-N Ratio.

the results, horizontal axis is the non-dimensionalized number by the reference value of the thrust stand A except c_1, c_2 and l_1/l_2 , and the vertical axis is the S-N ratio. When we calculated the S-N ratio, the value of the signal that originated with the only rotation motion, we can find this value from Eq. (1), is the first peak voltage, and the value of the noise that came from the motion other than the rotation motion is evaluated as the root mean square (RMS) value.

From this result, we can also find that the most effective parameters to increase the S-N ratio are: the moment of inertia of the main body J_2, the arm length of the thruster side l_t, and the distance from the rotational axis to the measurement point l_m. Figure 11 shows the design of the main body of the thrust stand B. To meet the conflictive request for a decrease the moment of inertia and an increase the arm length, we kept the rotational axis away from the thruster, and made the main body with the aluminum angles because of the light weight. We also put the measurement point near the thruster to get a long length from the rotational axis.

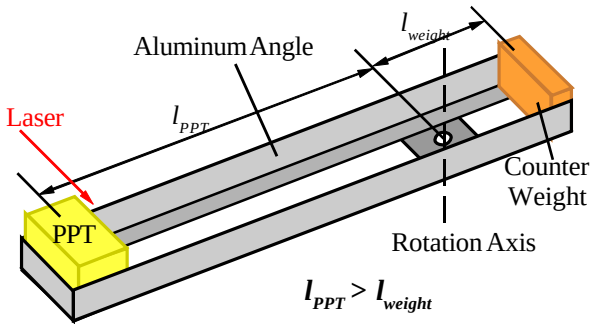

Fig. 11 Design of Main Body.

We also contrived the rotational axis. The rotational axis of the thrust stand A is a pair of wires, and the cables of the PPT put along the wires, but the restoring force of these cables cannot be ignored. We selected the pipe as the rotation axis and put these cables into the pipe. Furthermore, the rotation axis should be as small rotational spring constant as possible. According to the St. Venant theory, the torsional rigidity of open section is 1/3 times that of closed section. Considering this, we selected the C-section pipe as the rotational axis of the thrust stand B. This pipe has a outer diameter of 6mm, wall thickness of 0.5mm and a length of 300mm, and it is made from aluminum. The rotational spring constant can be found from the following equation.

$$k_t = \frac{T}{q} = \frac{GJ_s}{l} = \frac{G}{3l}\int_{S_l} t^3 ds = \frac{pdt^3 G}{3l} = 5.7\times10^{-2}\ \text{[Nm/rad]} \qquad (4)$$

T : torque, q : rotation angle, G : modulus of rigidity, J_s : polar moment of inertia of area, l : length, t : wall thickness, d : outer diameter

The schematic of the thrust stand B and the appearance of the experiment are shown in Fig. 5.

Calibration

The calibration was carried out by inelastic collision with the ball of known weight. Figure 12 exhibits the schematic of this method. The weight was suspended from the ceiling of the vacuum chamber with a thread having negligible weight, and fixed with the electromagnet before collision. When turned the switch of electromagnet off, the weight impacted with the thrust stand, and this impulse I_{cal} can calculate from Eq. (5). After the weight

$$I_{cal} = m\sqrt{2gl\left(1-\cos\tan^{-1}\frac{x}{l}\right)} \qquad (5)$$

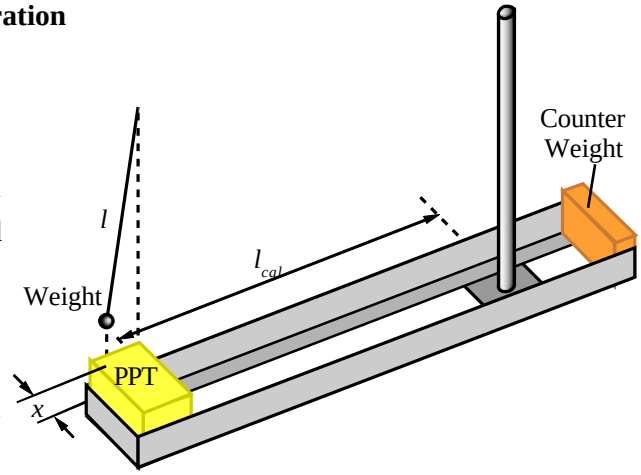

Fig. 12 Schematic of Calibration.

impacted with, stuck to the adhesive tape on the thrust stand to avoid reflecting, and integrated with the thrust stand. We measured the displacement of the thrust stand, and carried out the calibration. Figure 13 shows that result. The motion of the thrust stand B can be simulated with Eq. (6), and we also carried out the calibration by the simulation. Figure 13 also shows this result.

$$\begin{cases} J\ddot{q} + kq = 0 \\ \ddot{j} + \dfrac{g}{l} j = 0 \end{cases} \qquad (6)$$

$$q(0) = j(0) = 0,\ \dot{q}(0) = \frac{l_t I_b}{J},\ \dot{j}(0) = \frac{I_b}{ml}$$

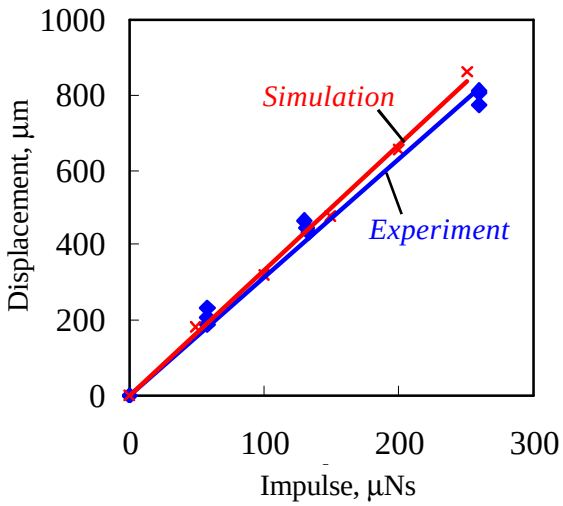

Fig. 13 Result of Calibration.

Target Pendulum

In Japan, most of small impulse measurements up to date have been performed by using a target pendulum[10]. We also measured the impulse bit of our coaxial PPT with such device. Figures 14 and 15 show the shape of the target called cylindrical target and the measurement system[11], respectively, we measured the displacement of the target with the laser displacement meter. To enhance multiple collisions inside this target, the target has a bottom cone and a many slits. The PPT is placed just in front of the target, the particles in the plume of PPT collide the bottom cone, and then the particles go through between slits engaging in a large number of collisions.

In measurement using the target pendulum, we made the displacement of the target amplified by multi-firing synchronized with the periodic motion of the target swing, and the calculated the single impulse.

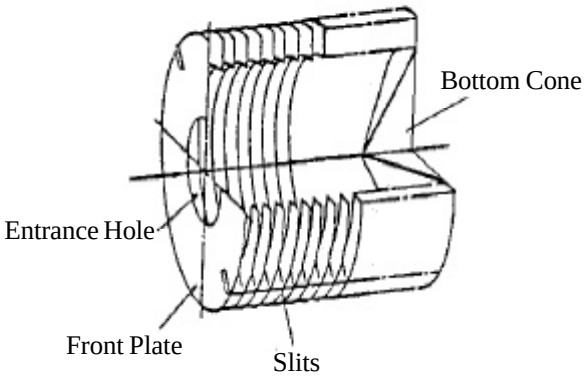

Fig. 14 Cylindrical Target.

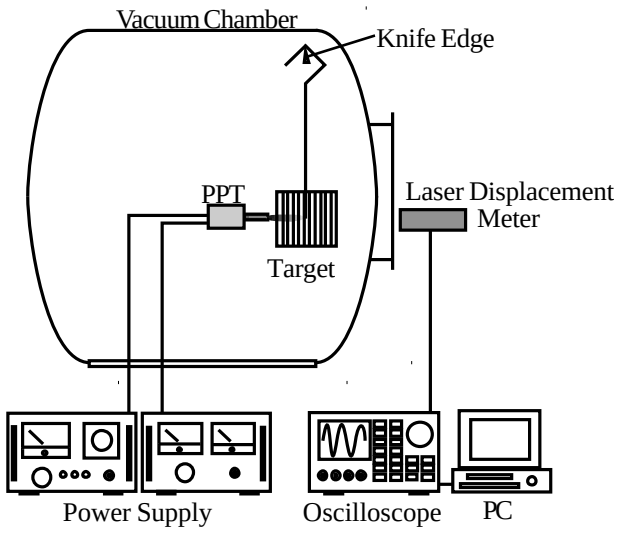

Fig. 15 Measurement System of the Target Pendulum.

Experimental Result

Figure 16 shows the displacement of the thrust stand B when the charge energy is 8.8J and 5.0J. Comparing this result with Fig. 6 showing the displacement of the thrust stand A at a charge energy is 19.6J, the improvement of the S-N ratio can be recognized.

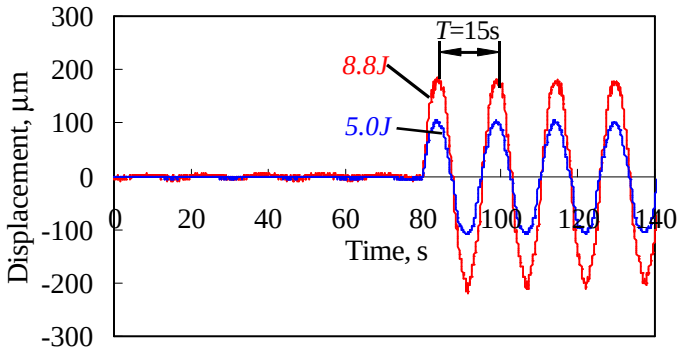

Fig. 16 Diplacement of Thrust Stand B.

Figure 17 shows the result of the impulse bit measurement with two methods: thrust stand B and target pendulum. Although a large difference between the measurement results of two kind of methods cannot be found, the target pendulum method has a tendency of overestimation a little more than the thrust stand method. The main reason is the effect of the elastic collision of the target pendulum. In measurement with the target pendulum, the target caught the plume of the PPT, so the effect of the elastic collision is unavoidable, and this effect may result in a small difference between the results of two methods.

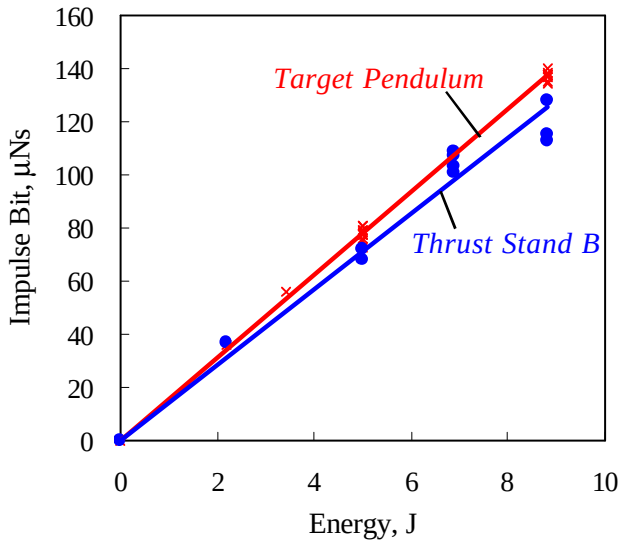

Fig. 17 Result of Two Measurement Methods.

Summary

A measurement system for the impulse bit of a coaxial PPT was built, and a torsion-type thrust stand suspended from the ceiling of the vacuum chamber was selected. The motion of this thrust stand was analyzed, and the dependency of the S-N ratio on a variety of parameters was found in order to get a satisfactory such ratio. Accordingly, a torsion-type thrust stand enabling the measurement of a single shot impulse was developed: this thrust stand has a C-section pipe as the rotation axis. We successfully measured the impulse bit of a coaxial PPT with the target pendulum, which is the conventional method of a small impulse measurement. And we also found that the result of the measurement with the target pendulum overestimates a little than that with the thrust stand, but that might be in a tolerable range.

Reference

1. Muller J., *Thruster Options for Microspacecraft: A Review and Evaluation of State-of-the-Art and Emerging Technologies*, vol. 187 of AIAA Progress in Astronautics and Aeronautics, chap. 3, AIAA, 2000.

2. Kumagai N., *et. al.*, "Research and Development Status of Low Power Pulsed Plasma Thruster System for μ-Lab Sat II," 28th International Electric Propulsion Conference, Toulouse, Fr., IEPC-03-202.

3. Rayburn, C., Campbell, M., "Development of a Micro Pulsed Plasma Thruster for the Dawgstar Nanosatellite," 36th Joint Propulsion Conference, Huntsville, Alabama, AIAA 2000-3256.

4. Koizumi H., *et. al.*, "A Thrust Stand for Liquid Propellant Pulsed Plasma Thrusters," 23rd International Symposium on Space Technology and Science, Matsue, Japan, ISTS 2002-b-13.

5. Gamero-Castaño M., *et. al.*, "A Torsional Balance that Resolves Sub-micro-Newton Forces," 27th International Electric Propulsion Conference, Pasadena, California, USA, IEPC-01-235.

6. Ziemer J. K., "Performance Measurements Using a Sub-Micronewton Resolution Thrust Stand," 27th International Electric Propulsion Conference, Pasadena, California, USA, IEPC-01-238.

7. Phipps C., *et. al.*, "Diode Laser-Driven Microthrusters : A New Departure for Micropropulsion," AIAA Journal, 40, No.2, February, 2002, pp.310-318.

8. Jamison A. J., "Accurate Measurement of Nano-Newton Thrust for Micropropulsion System Characterization," 27th International Electric Propulsion Conference, Pasadena, California, USA, IEPC-01-236.

9. Haag T. W., "Thrust Stand for Pulsed Plasma Thruster," Review of Scientific Instruments, 68(5), pp.2060-2067, 1997.

10. Yanagi R., *et. al.*, "A New Type Target for the Measurement of Impulse Bits of Pulsed Plasma Thrusters," 15th International Electric Propulsion Conference, Las Vegas, Nevada, USA, AIAA-81-0712.

11. Igarashi M., *et. al.*, "Performance Improvement of Pulsed Plasma Thruster for Micro Satellite," 27th International Electric Propulsion Conference, Pasadena, California, USA, IEPC-01-152.